The stopping power of hydrogen in hafnium and the importance of relativistic $4f$ electrons

C. C. Montanari,[1, *] P. A. Miranda,[2] E. Alves,[3, 4] A. M. P. Mendez,[1] D. M. Mitnik,[1]
J. E. Miraglia,[1] R. Correa,[2] J. Wachter,[2] M. Aguilera,[2] N. Catarino,[3] and R. C. da Silva[3]

[1]*Instituto de Astronomía y Física del Espacio, Consejo Nacional de Investigaciones Científicas*
y Técnicas - Universidad de Buenos Aires, Pabellón IAFE, 1428 Buenos Aires, Argentina
[2]*Departamento de Física, Facultad de Ciencias Naturales,*
Matemática y del Medio Ambiente. Universidad Tecnológica Metropolitana. 7800002, Chile
[3]*Centro de Ciências e Tecnologias Nucleares, Instituto Superior Técnico,*
Universidade de Lisboa, 2696-953 Sacavém, Portugal
[4]*Instituto de Plasma e Fusão Nuclear, Instituto Superior Técnico,*
Universidade de Lisboa, 2696-953 Sacavém, Portugal
(Dated: April 21, 2020)

The stopping power of protons through Hf foil has been studied both experimentally and theoretically. The measurements were performed at the Laboratory of Accelerators and X-Ray Diffraction in Lisbon by using the transmission method on self-supporting stopping material. The overall uncertainty of around 5% was established over the protons energy range (0.6-2.5) MeV. The theoretical developments involved fully relativistic atomic structure calculations for Hf, which required the solution of the Dirac equation. The shell-wise local plasma approximation (SLPA) was used to describe the energy transferred to the bound $1s$-$4f$ electrons, and the outer four electrons were considered as a free electron gas (FEG). We found the relativistic description of the $4f$-shell and the screening between $4f$ and $5p$ electrons to be decisive around the stopping maximum. Present theoretical and experimental results are in excellent agreement in the energy region of the new measurements. However, our theoretical stopping cross sections show substantial differences with the most used semi-empirical models (SRIM2013 and ICRU-49) at intermediate to low energies. Our calculations suggest the stopping maximum to be higher and shifted to lower energies than these previous predictions. Future measurements below 100 keV would be necessary for a better understanding of the stopping power around the maximum and below.

I. INTRODUCTION

For impact energies above a few keV/amu, mono-energetic charged particles penetrating a foil of any material lose their energy through a series of consecutive inelastic collisions, mainly with target electrons [1, 2]. The information given by the energy loss process is essential not only to have a better comprehension of the physics behind the fundamental interactions but also because it plays a vital role in many applied fields such as materials science, nuclear physics, ionic implantation, and radiotherapy [2, 3]. Experimental data on ion mean energy loss per unit path $S(E)$ is of crucial relevance to check the reliability of semi-empirical models and to determine some key parameters [4–6]. The experimental data available is often rather scarce, which is troublesome when the material under study corresponds to an element of low occurrence on the Earth's upper crust, such as hafnium.

So far, only one experimental work has been published regarding the stopping power cross section of pure hafnium for protons [7], while more attention has been recently given to studies involving hafnium oxide due to its practical use [8–11]. It is well known that signif-icant attention has been paid in recent years to transition metal-oxides such as HfO_2 because of their potential as alternative gate dielectrics to replace SiO_2 for the future generation of nano-electronics with less than 45 nm gate length [12, 13]. Some important physical properties of the above mentioned metal-oxide films depend on their thickness, which is often measured by using Rutherford Backscattering Spectrometry [14, 15]. This method relies heavily on the determination of the stopping power of ion beams in the material of interest.

In this study, we report experimental stopping power cross sections over the incident energy range (0.6-2.5) MeV for protons crossing self-supported Hf thin-film by using the transmission method. We aim not only to upgrade stopping power data compilations [16, 17] but also to provide useful information about the processes governing the slowing down of protons in multi-electronic targets. In the rare earth metals, the $4f$ electrons play an essential role in the stopping power since they belong to the first shell of bound electrons below the conduction band. As already noted [18], the free electron gas (FEG) shows unexpected behavior in these elements, which casts doubts on its proper description. In the case of Hf, we found the contribution of the $4f$-shell to be decisive even at impact energies around the stopping maximum, as will be shown later.

The theoretical approach implemented in this work uses the shell-wise local plasma approximation
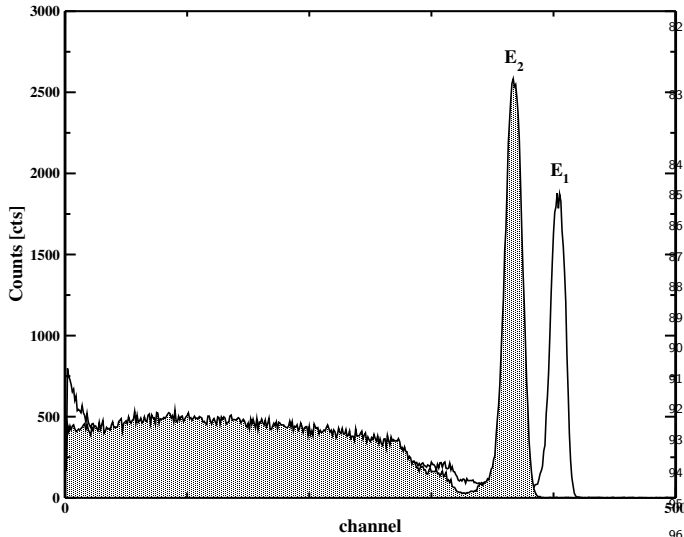
FIG. 1. RBS spectrum for $E_{\mathrm{avg}} = 921.1$ keV protons on the hafnium sample, which is subsequently used to determine the energy loss in the foil.

(SLPA) [19] to describe the energy transferred to the bound $1s$-$4f$ electrons and two different models for the FEG; in low energy region, the screened potential with cusp condition model (SPCC) [20], which is non-linear binary formalism, and the Mermin-Lindhard dielectric formalism (ML) [21] for energies around the stopping maximum and above. Our model requires the relativistic wave functions and binding energies of Hf and considers four electrons per atom in the FEG [22]. Hafnium is particularly interesting since the filled $4f$-subshell (with 14 electrons) is the main contributor below the FEG, causing the stopping cross sections to be very sensitive to a good description of this shell. The screening among the $4f$ and $5p$ electrons has been considered and found to play a significant role within the SLPA calculations.

The experimental details and data are given in Section II, while the theoretical method is explained in Section III. Present theoretical and experimental values are finally compared to the experimental values measured by Sirotinin *et al.* [7] with the backscattering method, the theoretical results by Grande and Schiwietz [23, 24], and by Sigmund and Schinner [25], and also with the semi-empirical values from the SRIM-2013 package [26] and the ICRU-49 tabulation [27]. Conclusions and discussions are given in Section V. All the present data can be found at the Zenodo platform [28].

II.   EXPERIMENTAL ARRANGEMENTS

A.   Accelerator and scattering Chamber

The procedure used in this work to obtain stopping power data is essentially the same as described in Ref. [29]. The present measurements were made at the IST/LATR (Laboratory of Accelerators and X-Ray Diffraction) in Lisbon. This facility uses a 2.5 MV Van de Graaff accelerator to deliver ^{1}H^{+} primary ion beams through a series of electrostatic lenses and collimators onto a thin Au/SiO$_2$ sample, which is used as a scattering center. This sample was placed in the center of an RBS/C scattering chamber, where a high vacuum (pressure of $\sim 10^{-6}$ Torr) was maintained during the measurements. The beam current on the sample was kept at around 5.0 nA to attain sufficient statistics in each particle spectrum. By using a beam spot of about 1.0 mm in diameter, a solid angle of 11.4 msr was attained. The overall energy resolution (FWHM) of the detection system was about 15 keV relative to 5.486 MeV alpha particles from a ^{241}Am source.

B.   Target

The stopping material under analysis was a hafnium foil with a nominal thickness of 1.0 μm and 99.95% purity, which was supplied by Lebow Company [30]. However, a more precise thickness value was achieved by measuring the energy loss of alpha particles coming from a calibrated (^{239}Pu, ^{241}Am, ^{244}Cm) source. From the alpha spectra with and without the Hf foil interposed, the characteristic energy shift δE was measured and then combined with the stopping power for 5.486 MeV alphas on hafnium (55.69 eV/10^{15} at/cm^2) found in Ref. [26] to obtain an areal density of $(4.13 \pm 0.21) \times 10^{19}$ at/cm^2, which corresponds to a thickness of $0.920 \pm 0.046\mu$m.

C.   Energy loss measurement

Once the beam impinges on the Au/SiO$_2$ sample, protons are backscattered towards a Si surface barrier detector located at $140°$ relative to the initial beam direction. Fig. 1 shows two particle spectra, where the ion energies E_2 and E_1 are associated with a placed and removed hafnium sample, respectively. Both energy distributions were fitted by Gaussian functions to obtain the mean energy and width (FWHM) of the peaks [31], and from the difference between these two peak positions in the spectrum, the total energy loss $\Delta E = (E_1 - E_2)$ in the foil was calculated. As established in previous studies [5, 29], the experimental stopping power cross sections $\varepsilon(E)$ are determined at some mean energy E_{avg} by measuring the ion energy losses ΔE within the investigated Hf foil, which has a mean thick-

ness denoted by Δx. In this way, only when the energy loss fraction $\Delta E/E_{\text{avg}}$ across the Hf foil is not exceeding 20%, it is possible to define the stopping cross section by [32, 33]:

$$\varepsilon(E) = \frac{S(E)}{N} = -\frac{dE}{N\,dx} \approx -\frac{\Delta E}{N\Delta x}, \qquad (1)$$

where N denotes the atomic number density (atoms cm^{-3}) of the material under study. When this condition was not fulfilled, a small correction to the mean energies E_{avg} was applied in order to account for the non-linear dependence on ion energy of stopping powers [34, 35].

III. THEORETICAL METHOD

The energy loss of ions in metal targets responds to different physical mechanisms, depending on the impact ion velocity. At low velocities, the binary collisions are responsible for the loss of energy by the ion. The main contribution is the ionization of electrons of the metal conduction band, which is well approximated by a free electron gas (FEG) of Fermi velocity v_F. Above a particular velocity value (i.e., $v \geq 1.5\,v_F$), not only binary but also collective excitations (plasmons) occur [20]. Moreover, at high energies, also the bound electrons contribute to the stopping power. The method used in this work combines a FEG description for the interaction with the valence (or conduction) electrons, and a different one for the interaction with the bound electrons.

We used the SPCC model [20] to describe the stopping power of low velocity charged particles in the FEG. It is a non-perturbative binary collisional approximation, thus valid at energies below that of plasmon excitations. The SPCC [20] is based on a screened central potential with cusp condition of the electronic density close to the projectile. This model proved to give a good description of the induced electron density even for negative projectiles [20] and reproduces the low velocity proton-antiproton differences in the stopping power (Barkas effect). The SPCC formalism only depends on the Wigner-Seitz radio, r_S, which is a measure of the electronic density of the FEG. For metals of well-known r_S, the SPCC describes the low energy experimental stopping data correctly [20], agreeing with the DFT results by Echenique and coworkers [36, 37] at $v = 0$.

Hafnium ($Z = 72$, [Xe] $4f^{14}\,6s^2\,5d^1_{3/2}\,5d^1_{5/2}$) belongs to the first groups of transition metals, with four electrons as FEG ($r_S = 2.14$ a.u.) and $1s$-$4f$ electrons bound. We compared the computed r_S with the experimental value obtained from the measured energy loss function by Lynch et al. [38]. The experimental plasmon energy of Hf is $\hbar\omega_P \approx 15.8$ eV, with a width at half maximum $\delta \approx 4.4$ eV, and $r_S \approx 2.07$ a.u. [38]. The difference of less than 5% between theo-

retical and experimental r_S assess Hf as a canonical target [20].

Above certain impact velocity, the plasmon contribution is essential (i.e., around and above the stopping maximum). A value of interest for our analysis is the minimum impact velocity to excite plasmons, v_P. In the dielectric formalism, this value can be obtained as $v_P \approx v_F[1 + (3\pi\,v_F)^{-1/2}]$ [39]. To describe the energy loss considering collective and binary excitation, we resort to the ML dielectric formalism [21], which is a linear response, perturbative approximation, so it depends on the square of the ion charge. In this formalism, the response of target electrons to the ion passage is described through the quantum dielectric function, which depends on the characteristic r_S and δ parameters of the FEG.

For the stopping power due to bound electrons, the SLPA [19, 20] is employed. It is worth mentioning that the only inputs for the SLPA are the space-dependent densities of each shell in the ground state, and their binding energies. Collective processes and screening among electrons are included. Since hafnium is a relativistic target, the wave functions and binding energies must be obtained by solving the many-electron Dirac Hamiltonian. Details of these calculations and a table of binding energies have been published in Ref. [22], while Slater-type orbital expansions are given in Ref. [40].

To assess the importance of a fully relativistic description of bound electrons, Fig. 2 (a) shows our binding energies, $E_{nl\pm}$, with $\pm = j\pm1/2$; and (b) the relative errors with respect to the non-relativistic values [41]; and experimental data on solid-state Hf [42], which is available only for $1s$ to $4f_\pm$ subshells, as expected. We notice that not only the most inner shells require relativistic calculations, but also the outer $5p$ and $4f$ shells. Furthermore, this figure shows very clearly the disability of non-relativistic calculations to describe the experimental data, which surprisingly worsens from the inner to the outer shells.

From the comparison with the experimental values in Fig. 2 (a), it can be noted that the sign of the binding energy deviations is inverted for the outer $5s$ and $4f$ electrons, with the experimental binding energies being less bounded than our theoretical ones. Small differences for the outer shells are expected since the experimental values correspond to hafnium in solid-state, while our theoretical calculations correspond to the element in the gas phase.

More detail of the theoretical binding energies is given in Fig. 2 (b), where relative errors with respect to the experimental values are shown. This figure shows clearly that the relativistic corrections are critical to describing the atomic structure of hafnium, even for the outer shells. It turns out that the errors committed in the non-relativistic calculations of the inner shell orbitals propagate, through the Hartree-Fock approximation, to
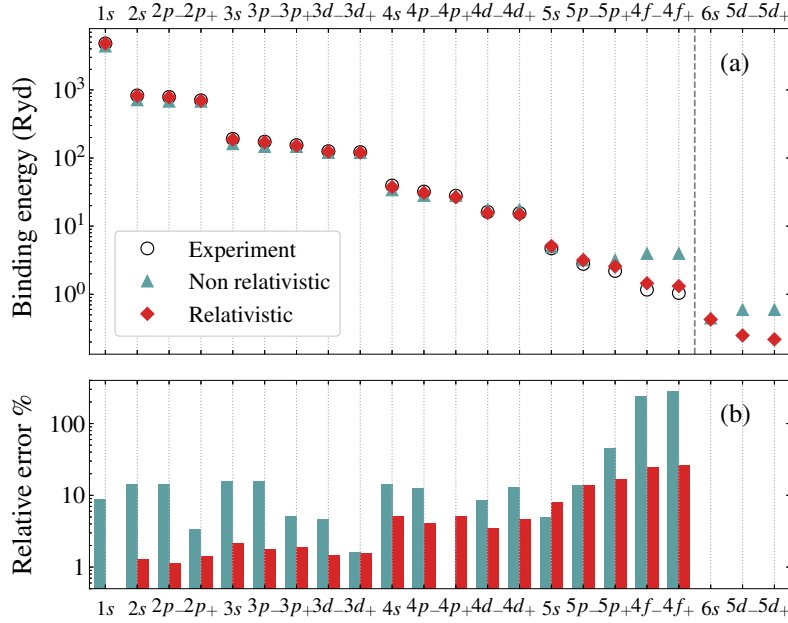
FIG. 2. (a) Binding energies of Hf. ~~Non-relativistic and~~ Present relativistic ~~calculations~~ and available non-relativistic [41] values are given with filled symbols. Experimental measurements for solids [42] are depicted with ~~hollow~~ open circles. (b) Corresponding relative errors with respect to experimental data.

the outer shells. The importance of fully relativistic calculations for the outer shells has already been noted for Au, Pb, Bi, and W [43].

For the contribution of bound electrons to the total stopping cross sections, the SLPA considers independent contributions of each subshell. Our relativistic binding energies present spin-orbit split. However, in total stopping power, where the initial state of the excited electron is not measured, the quantum uncertainty in energy ΔE melts this split. The ~~criteria~~ criterion $\Delta E \Delta t \geq \hbar/2$ merges the energies $E_{nl+} - E_{nl-}$ for sufficiently small values of Δt (the collisional mean-time). In fact, at sufficiently high impact velocity, we can expect all target electrons to respond together to the ion passage [44, 45]. Following previous ~~work~~ works [43], the collisional time is estimated as $\Delta t \approx \langle r_i \rangle / v$, with $\langle r_i \rangle$ and v being the orbital mean radio and impact velocity, respectively.

~~Theoretical total stopping cross sections of protons in hafnium adding FEG and bound 1s-4f contributions, as mentioned in the inset. The vertical grey dashed-line indicates the energy above which plasmon excitation is possible. The SLPA total stopping values for 1s-4f bound electrons with and without 5p-4f screening are displayed with solid and dotted lines, respectively.~~

~~The SLPA calculates the contribution of each subshell of bound electrons to the total stopping cross sections. We~~ In the case of hafnium, we found that for every subshell of ~~Hf, at the impact energy at which this sub-shell began to contribute~~ electrons, the spin-orbit split ~~was unresolved . Then~~ is unresolved in the energy region this

sub-shell contributes. Therefore, the nl-electrons should be considered together, responding to the ion passage as a single gas of electrons with density $\delta_{nl}(r)$ and ~~a~~ mean binding energy E_{nl}. This feature is ~~important~~ vital within the SLPA calculations because it accounts for the screening among electrons of the *same* binding energy. For example, the $4f_-$ and $4f_+$ of Hf can only be resolved for impact energies $E < 0.05$ keV, but the contribution of $4f$ to the total stopping is negligible for $E < 40$ keV. Moreover, the $5p$ and $4f$ electrons of Hf are very close in energy ($\Delta E_{5p-4f} \approx 1$ a.u. [22]), and they react together ~~for~~ at impact energies $E > 40$ keV (inter-shell screening). As already mentioned, at higher energies, inter-shell screening is possible for other subshells (i.e., $4p$-$4d$ for impact energies above 0.9 MeV), but its weight in the total stopping is minor for deeper shells.

Finally, in all our calculations [20], we assumed the projectile to be proton and not neutral hydrogen. When an ion moves inside a metal, the FEG screens the nucleus, so the binding energies will be smaller than outside the metal, and this effect is more critical at low impact velocities v. In the case of hydrogen, the difference is drastic, i.e., for H inside Hf ($rs = 2.07$), the $1s$-bound state is almost null at $v < 2$ [39]. It is worth to mention that this assumption agrees with Ziegler SRIM code [26] but differs from CasP code [23], that predicts neutral hydrogen at very low velocities.

In Fig. 3, we display the present theoretical stopping cross section of Hf for protons using the relativistic wave functions and binding energies, but with and without the
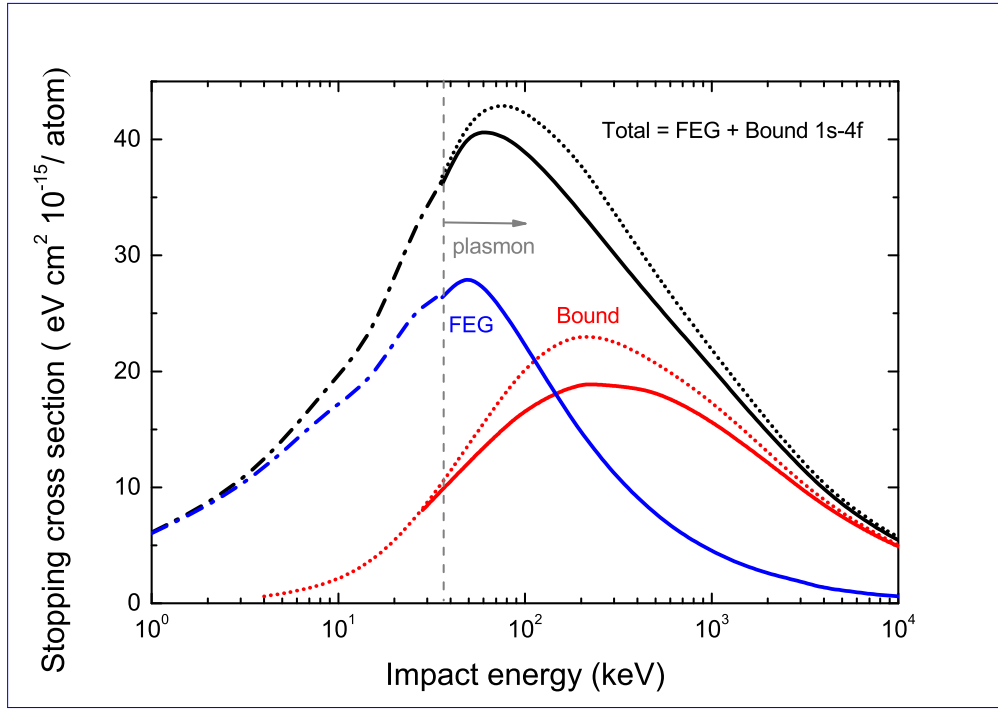
FIG. 3. ~~Stopping power~~ (color online) Theoretical stopping cross ~~section~~ sections of ~~hafnium for~~ protons in hafnium. ~~Symbols: solid circles~~Blue dash-dotted-line, ~~present values~~the non-perturbative SPCC for the FEG; ~~open circles, previous data [7]. Curves: Black~~blue solid-line, ~~present full theoretical~~ ML results for the FEG (includes plasmon excitation); red solid and dotted-lines, the SLPA results for bound electrons with ~~4f~~and without $5p$-$4f$ screening~~; violet dashed-line,~~ ~~values from ICRU-49 [27]~~ respectively. Black curves, total stopping adding the FEG and ~~green dotted line~~bound $1s$-$4f$ contributions: dash-dotted-line, ~~SRIM-2013 [26]~~SPCC (FEG) + SLPA (bound); solid-line, ML (FEG) + SLPA (bound) with 4f-5p screening; dotted-line, ML (FEG) + SLPA (bound) without 4f-5p screening. The vertical grey dashed-line indicates the energy of 37 keV above which plasmon excitation is possible.

301 $5p$-$4f$ screening. We ~~added~~ show the FEG and ~~the~~ bound
302 electron contributions ~~as explained above~~separately and
303 the total stopping as the addition of both of them. The
304 minimum energy for plasmon excitation was estimated ~~to~~
305 at approximately 37 keV. We used the non-perturbative
306 SPCC model for impact energies $E \leq 37$ keV, and the
307 perturbative ML calculation above this ~~energy. Clearly,~~
308 ~~considering~~ value. Bound $1s$-$4f$ electrons (relativistic
309 wave functions and binding energies) are calculated
310 with the SLPA and shown separately in Fig. 3 with
311 and without the $4f$-$5p$ screening. Below ~ 40 keV,
312 the difference between both calculations is negligible.
313 Considering $5p$-$4f$ electrons as a single group of 20 elec-
314 trons with screening among them gives lower stopping
315 values than the addition of the separate $5p$ and $4f$ con-
316 tributions. Notice that this shell correction can ~~only be~~
317 ~~considered within a many electron model~~be considered
318 naturally within a many-electron model, such as the
319 SLPA.

IV. ANALYSIS OF THE RESULTS AND DISCUSSION

320 The present data ~~and theoretical results~~ are displayed
321 in Table I~~, and Fig. 4~~. As can be ~~seen in Table I~~observed,
322 an overall relative uncertainty of around 5% was achieved
323 for the experimental stopping power values, which are
324 mainly due to the uncertainty in the hafnium foil thick-
325 ness.
326 ~~In~~ Fig. 4 ~~, we have good~~ synthesizes the results
327 of the present work. The agreement between the
328 present theoretical results and the new measurements
329 displayed in Table I is excellent. Present measurements
330 using the transmission method are in good agreement
331 with the previous data by Sirotinin [7], which were
332 measured in backscattering geometry. Our theoreti-
333 cal approach also agrees with ~~previous~~ the data by
334 Sirotinin [7], except for the lowest energy measure-
335 ment at 80 keV. ~~It is interesting that~~ We have also
336 included in this figure the theoretical curves from the
337 CasP5.2 code by Grande and Schiwietz [23, 24] and
338 from the DPASS code by Sigmund and Schinner [25]
339 , both available online. Furthermore, we incorporated
340 the semi-empirical results from SRIM-2013 [26] and the
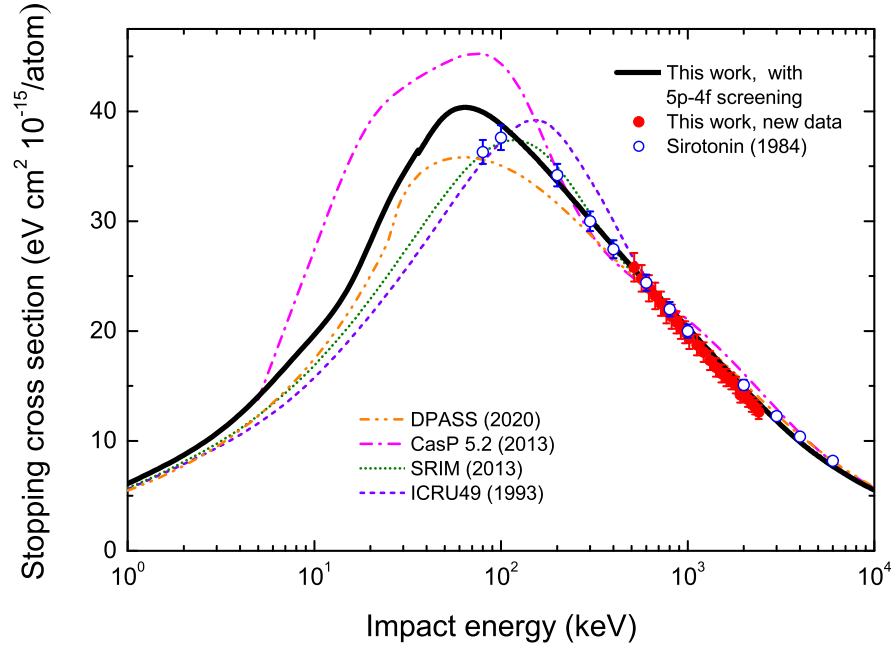341 ICRU49 tables [27]. Interestingly, our full theoretical

FIG. 4. (color online) Stopping power cross section of hafnium for protons. Symbols: solid circles, present values; open circles, previous data [7]. Curves: Black solid-line, present full theoretical results with $4f$-$5p$ screening; pink dash-dot line, theoretical CasP5.2 [23, 24] values; orange dash-double-dot line, theoretical DPASS [25] results; green dotted-line, semi-empirical SRIM-2013 [26]; violet dashed-line, ICRU49 [27] tabulated values.

TABLE I. Stopping power values S_{exp} of hafnium for protons measured in this work. $\Delta E/E$ values are also shown.

E_{avg} keV	S_{exp} eV/(10^{15} at/cm^2)	$\Delta E/E$ %	E_{avg} keV	S_{exp} eV/(10^{15} at/cm^2)	$\Delta E/E$ %	E_{avg} keV	S_{exp} eV/(10^{15} at/cm^2)
516.6	25.8 ± 1.3	20.5	1170.3	18.25 ± 0.91	6.4	1813.4	15.10 ± 0.76
567.8	24.8 ± 1.2	17.9	1220.0	18.08 ± 0.90	6.1	1862.7	14.79 ± 0.74
618.8	23.9 ± 1.2	15.8	1269.6	17.57 ± 0.88	5.7	1912.0	14.21 ± 0.71
669.6	23.2 ± 1.2	14.2	1319.2	17.32 ± 0.87	5.4	1961.2	14.46 ± 0.72
720.1	22.5 ± 1.1	12.8	1368.8	17.15 ± 0.86	5.1	2010.4	14.34 ± 0.72
770.5	21.8 ± 1.1	11.6	1418.3	16.69 ± 0.83	4.8	2059.6	13.76 ± 0.69
820.8	21.3 ± 1.1	10.7	1467.8	16.43 ± 0.82	4.6	2108.8	13.78 ± 0.69
871.0	20.8 ± 1.0	9.8	1517.2	16.13 ± 0.81	4.4	2158.0	13.70 ± 0.69
921.1	20.3 ± 1.0	9.1	1566.7	16.04 ± 0.80	4.2	2206.5	13.33 ± 0.67
971.1	19.9 ± 1.0	8.4	1616.0	15.77 ± 0.79	4.0	2256.4	13.27 ± 0.66
1021.0	19.33 ± 0.97	7.8	1665.4	15.51 ± 0.78	3.8	2305.5	13.07 ± 0.65
1070.8	19.03 ± 0.95	7.3	1714.8	15.46 ± 0.77	3.7	2354.7	12.91 ± 0.65
1120.6	18.73 ± 0.94	6.9	1764.1	14.93 ± 0.75	3.5	2403.8	12.61 ± 0.63

curve differs from SRIM-2013 for impact energies below 100 keV. We obtain a stopping maximum of approximately 40×10^{-15} eV cm^2/atom at 65 keV. Instead, following the up-to-now only set of data –[7], SRIM-2013 suggests a lower stopping maximum at an impact energy of 115 keV. The stopping maximum is a susceptible region for any full theoretical description without parameters, and this is quite visible in a linear-scale plot like Fig. 4. However, the impact energy for the maximum seems to agree between our curve and DPASS, although it is 10% below. Instead, CasP a maximum value of the stopping power 10% above

our value and a completely different shape at lower energies. It is worth mentioning that ~~similar theoretical~~ our model gives similar results using the experimental value $r_S = 2.07$ a.u. ~~instead of the theoretical~~ rather than the theoretical one $r_S = 2.14$ a.u. ~~give~~, with the stopping maximum at the same impact energy but 4% higher.

Future experiments for impact energies below 100 keV would be ~~important~~ essential to complete this study ~~on~~ the stopping of Hf for protons. In the energy region $80 - 500$ keV, only the measurements by Sirotinin's group [7] from 1984 are available. SRIM-2013 includes these values in the code fitting, so it does not represent a test for this data. Undoubtedly, new measurements are needed in three specific energy regions: below 500 keV, around the stopping maximum (i.e., $50 - 200$ keV), and at low impact energies.

V. CONCLUSION

In this work, we have used the transmission method to experimentally determine stopping power cross section values for (0.6-2.5) MeV protons incident on self-supporting Hf foils with an overall uncertainty of around 5%. Additionally, we calculated values extracted from the theoretical framework that involved the relativistic wave functions and binding energies of Hf ~~, and considered 4~~ and considered four electrons per atom in the free electron gas. The shell-wise local plasma approximation was employed to describe the energy transferred to the bound $1s$-$4f$ electrons, and two different models for the FEG: the screened potential with cusp condition (SPCC model) for energies below that of the plasmon excitation, and the Mermin-Lindhard dielectric formalism, for energies around the stopping maximum and above. Present theoretical stopping cross sections cover an extensive energy range from 1 keV/~~amu 10 meV~~amu to 10 MeV/amu.

At high impact energies, the new stopping measurements are in good agreement with our theoretical results, with previous experimental data and semi-empirical values by SRIM-2013 and ICRU-49. However, we call the attention that around the stopping maximum and at lower impact energies, the difference between our full-theoretical results and SRIM is substantial. We compare our theoretical results with two other models given by the DPASS and CasP5.2 codes. Differences can be noted at intermediate to low impact energies, but they also support a stopping maximum at lower energy than SRIM predictions.

To the best of our knowledge, these are the first theoretical calculations of stopping in Hf ~~taking into account the atomic relativistic effect~~to take into account relativistic effects in the atomic structure and screening among electrons in a consistent way, from very low to high impact energies. Future experiments for impact energies ~~below 100 keV would be important to complete this study.~~ around the stopping maximum and in the low energy region would be essential to have a better understanding of the stopping of protons in hafnium.

[1] W.K. Chu, J.W. Mayer, and M.A. Nicolet ~~(Eds.)~~ ~~Backscattering Spectrometry,~~, *Backscattering Spectrometry* (Academic Press, New York, ~~1978.~~ 1978).

[2] P. Sigmund, ~~"Particle Penetration and Radiation Effects. General Aspects and Stopping of Swift Point Charges".~~ *Particle Penetration and Radiation Effects. General Aspects and Stopping of Swift Point Charges.* (Springer Series in Solid-State Sciences, ~~Vol. 151,~~ Springer, Berlin~~,~~ 2006)~~.~~, Vol. 151.

[3] D. Schardt, T. Elsässer, D. Schulz-Ertner, Rev. Mod. Phys. **82**, 383-425 (2010).

[4] P.K. Diwan, S. Kumar, Nucl. Instr. and Meth. B **359**, 78-84 (2015).

[5] D. Moussa, S. Damache and S. Ouichaoui, Nucl. Instr. and Meth. B **268**, 1754-1758 (2010); **343**, 44-47 (2015).

[6] S. Damache, S. Ouichaoui, A. Belhout, A. Medouni and I. Toumert, Nucl. Instr. and Meth. B **225**, 449-463 (2004).

[7] E.I. Sirotinin, A.F. Tulinov, V.A. Khodyrev, V.N. Mizgulin, Nucl. Instr. and Meth. B **4**, 337-345 (1984).

[8] I. Abril, M. Behar, R. Garcia Molina, R.C. Fadanelli, L.C.C.M. Nagamine, P.L. Grande, L. Schünemann, C.D. Denton, N.R. Arista, E.B. Saitovich, Eur. Phys. J. D 54, 65-70 (2009).

[9] M. Behar, R.C. Fadanelli, I. Abril, R. Garcia-Molina, C.D. Denton, L.C.C.M. Nagamine, N.R. Arista, Phys. Rev. A **80**, 062901 (2009).

[10] D. Primetzhofer, Nucl. Instr. and Meth. B **320**, 100-103 (2014).

[11] D. Roth, B. Bruckner, G. Undeutsch, V. Paneta, A.I. Mardare, C.L. McGahan, M. Dosmailov, J.I. Juaristi, M. Alducin, J.D. Pedarnig, R.F. Haglund, Jr., D. Primetzhofer, and P. Bauer Phys. Rev. Lett. **119**, 163401 (2017).

[12] J.H. Choi, Y. Mao, J.P. Chang, Mat. Sci. Eng. R **72**, 97-136 (2011).

[13] J. Robertson, R.M. Wallace, Mat. Sci. Eng. R **88**, 1-41 (2015).

[14] Z.B. Alfassi, "Non-destructive elemental analysis", Blackwell Science Ltd. (*Non-destructive elemental analysis* (Blackwell Publishing, Oxford, 2001).

[15] J.R. Tesmer, M. Nastasi, J.C. Barbour, C.J. Maggiore and J.W. Mayer, "Handbook of Modern Ion Beam Material Analysis", *Handbook of Modern Ion Beam Material Analysis.* (Materials Research Society, Pittsburgh, 1995).

[16] https://www-nds.iaea.org/stopping/.

[17] C.C. Montanari, and P. Dimitriou, Nucl. Instr. and Meth. B **408**, 50-55 (2017).

[18] D. Roth, B. Bruckner, M. V. Moro, S. Gruber, D. Goebl, J. I. Juaristi, M. Alducin, R. Steinberger, J. Duchoslav, D. Primetzhofer, and P. Bauer, Phys. Rev. Lett. **118**, 103401 (2017).

[19] C.C. Montanari and J.E. Miraglia , Adv. Quant. Chem. **65** in *Advances in Quantum Chemistry*, edited by Dz. Belkic D. Belkić (Elsevier, Amsterdam, 2013), Vol 65, Chap. 7, pp. 165-201.

[20] C.C. Montanari, and J.E. Miraglia, Phys. Rev. A **96**, 012707 (2017).

[21] N.D. Mermin, Phys. Rev. B **1**, 2362 (1970).

[22] A.M.P. Mendez, C.C. Montanari, D.M. Mitnik, Nucl. Instrum. Meth. B **460**, 114-118 (2019). ICRU report 49, Stopping Powers and Ranges for Protons and Alpha Particles, International Commission on Radiation Units and Measurements, 1993.

[23] G. Schiwietz, P. L. Grande, Nucl. Instrum. Meth. B **175-177**, 125-131 (2001); CasP code, available from www.casp-program.org

[24] G. Schiwietz and P. L. Grande, Nucl. Instr. and Meth. B **273**, 1-5 (2012); P.L. Grande and G. Schiwietz, Phys. Rev. A **58**, 3796 (1998).

[25] A. Schinner, P. Sigmund, Nucl. Instrum. Meth. B **460**, 19 (2019); P.Sigmund, A. Schinner, Eur. Phys. J. D **12**, 425 (2000). DPASS code, available from https://www.sdu.dk/en/DPASS/

[26] J.F. Ziegler, J.P. Biersack, M. D. Ziegler, *SRIM, The Stopping and Range of Ions in Matter*, (SRIM Co. Maryland, USA, 2008); SRIM2013, Computer Program and Manual. Available from www.srim.org.

[27] ICRU report 49, *Stopping Powers and Ranges for Protons and Alpha Particles*, International Commission on Radiation Units and Measurements (1993).

[28] C.C. Montanari *et al.* DOI: 10.5281/zenodo.3678785

[29] P.A. Miranda, A. Sepúlveda, J.R. Morales, T. Rodriguez, E. Burgos, H. Fernández, Nucl. Instr. and Meth. B **318**, 292-296 (2014).

[30] Lebow Company. 5960 Mandarin Ave. Goleta CA, 93117, USA.

[31] G. Sun, M. Döbelli, A.M. Müller, M. Stocker, M. Suter and L. Wacker, Nucl. Instr. and Meth. B **256**, 586-590 (2007).

[32] J. Raisanen, U. Watjen, A.J.M. Plompen, F. Munnik, Nucl. Instr. and Meth. **B** 118, 1-6 (1996).

[33] F. Schulz and J. Shchuchinzky, Nucl. Instr. and Meth. B **12**, 90-94 (1985).

[34] A.B. Chilton, J.N. Cooper and J.C. Harris, Phys. Rev. **93**, 413-418 (1954).

[35] M. Rajatora, K. Vakevainen, T. Ahlgre, E. Rauhala, J. Raisanen, K. Rakennus, Nucl. Instr. and Meth. B **119**, 457-462 (1996).

[36] P. M. Echenique, R. M. Nieminen and R. H. Ritchie, Sol. State Comm. **37**, 779-781 (1981).

[37] I. Nagy, A. Arnau, P. M. Echenique, and E. Zaremba, Phys. Rev. B **40**, 11983 (1989).

[38] D. W. Lynch, C. G. Olson, and J. H. Weaver, Phys. Rev. B **11**, 3617-3624 (1975).

[39] C. C. Montanari, J. E. Miraglia, and N. R. Arista, Phys. Rev. A **62**, 052902 (2000).

[40] A.M.P. Mendez, C.C. Montanari, D.M. Mitnik, *Slater-type orbital expansion of neutral hafnium, numerical solution of the relativistic Dirac equation*, available soon in arXiv.org.

[41] N. R. Badnell, Comput. Phys. Commun. , 182(7), 1528-1535 **182**, 1528 (2011).

[42] G. Williams in http://xdb.lbl.gov/Section1/Sec_1-1.html

[43] C.C. Montanari, D.M. Mitnik, C.D. Archubi, and J.E. Miraglia, Phys. Rev. A **70**, 032903 (2009); Phys. Rev. A **80**, 012901 (2009).

[44] J. Lindhard, M. Scharff, Mat. Fys. Medd. Dan. Vid. Selsk **27**, 1 (1953).

[45] W. K. Chu, D. Powers, Rev. Lett. A **40**, 23 (1972). C.C. Montanari, D.M. Mitnik, C.D. Archubi, and J.E. Miraglia, Phys. Rev. A **80**, 012901 (2009).